An Optimal Control Strategy for Crop Growth in Advanced Life Support Systems*

D. Fleisher† and H. Baruh‡
Rutgers University, New Brunswick, New Jersey, U.S.A.

September 21, 2000

Abstract

An elementary method for controlling crop growth in Advanced Life Support Systems is presented. Two models for crop growth are considered, one developed by the agricultural industry and used by the Ames Research Center, and a mechanistic model, termed the Energy Cascade model. Two control laws are applied to both models using wheat as the crop. A variety of circumstances are considered, such as model errors, measurement errors, and the incapability of applying the desired control input. It is shown that the proposed approach is a potentially viable way of controlling crop growth.

Keywords: Advanced Life Support, crop growth, mathematical modeling, optimal control.

Content Sentence: A method for controlling crop growth in Advanced Life Support Systems is introduced. Feedback control is used to compensate for perturbations in light intensity and model errors.

1 Introduction

Future manned space exploration will require life support systems that are independent of the earth for re-supply of food and resources. Integrated physical, chemical, and biological systems may provide mass closure for life support through recycling and recovery of system resources via waste processing, atmospheric purification, and food production for crew members from plant biomass production chambers. NASA (National Aeronautics and Space Administration) researchers are developing aspects of this system through the ALS (Advanced Life Support) program (15), (17), (20), (13).

Plant growth is expected to play an important role in ALS. Growth of higher plants provides crew members with food, potable water via transpiration, atmospheric gas exchange through photosynthesis, and a contribution to waste processing/resource recycling through hydroponic nutrient uptake. A mix of 8 to 14 crops is required to satisfy crew nutrition demands (16).

*Supported by NJ-NSCORT: New Jersey - NASA Specialized Center of Research and Training. N.J. Agricultural Experiment Station Paper # P-7501-07-00. Also, supported by NASA Graduate Student Researchers Program fellowship.

†Bioresource Engineering, 20 Ag Extension Way, New Brunswick, N.J. 08901-8500, (732)932-9753, fleisher@bioresource.rutgers.edu

‡Dept. of Mechanical and Aerospace Engineering, 98 Brett Road, Piscataway, N.J. 08854-8058, (732)445-3680, baruh@jove.rutgers.edu - corresponding author.

Crops in an ALS environment will most likely be hydroponically grown in individualized growth chambers with control over irradiance (photosynthetic photon flux or PPF), photoperiod, air temperature, relative humidity, CO_2 and O_2 concentrations, and nutrient delivery system quality (3). The environmental setpoints for each of these inputs should be selected to produce the desired levels of plant growth that satisfy ALSS production scheduling (i.e., timing and yield of each crop) for each crop. Production schedules would initially be derived from crew nutrition demands. Disturbances and system failures can influence plant production in a closed environment. These include poor crop seed germination, spread of plant pathogens and/or disease, and perturbations in environmental conditions in the growth chamber (12). Environmental perturbations can be of either short (less than 1 day) or long term duration, and may ensue from deliberate actions (to modify plant transpiration or photosynthetic rates to offset activities in other ALSS compartments, for example) or system failures (such as fluctuations in power availability or mechanical problems). In either case, crop growth, and hence production scheduling, may be adversely affected by environmental perturbations. This can negatively affect reliability and persistence issues for an ALS system (14).

Control strategies able to compensate for the effects of environmental perturbations on plant growth would be useful for ALS. However, most growth chamber controllers work to maintain static setpoints. These setpoint values are typically derived from heuristic knowledge and empirical studies for each particular crop (e.g. (7), (6), (18)). As a result, environmental control of growth chambers tends to concentrate on maintaining current setpoints at their predetermined levels; thus, environmental disturbances and their effects on the plant are not incorporated into the control. Optimization techniques have also been used to identify appropriate setpoint values. Modern greenhouse control integrates mathematical models of the greenhouse environment with simple plant growth models to prescribe daily environmental conditions. The result are management tools and control systems which dynamically determine optimal setpoints usually with the intention of increasing crop yield, quality, or decreasing energy consumption (e.g. (2), (1), (8), (9), (21), (22)). Chun and Mitchell (10) developed a dynamic controller that varied PPF to control lettuce canopy net photosynthesis in a growth chamber based on real time measurements of canopy gas exchange. In this case, the environmental input was dynamically varied so that the desired plant growth rate could be obtained. Such systems could be adapted for ALSS use, where controllers can both maintain setpoints and adjust them when necessary based on the measured or predicted state of the plant. Measurement errors and uncertainties in the mathematical models would need to be considered in developing this control.

In this paper, we propose to use feedback control to compensate for the effects of environmental disturbances in crop growth chambers by adjusting PPF to maintain desired crop growth rates. We consider two generic crop growth models and we develop two model-based feedback controllers, using wheat as the crop. Small-order mathematical errors are considered. The controllers are evaluated with several scenarios simulating short-term environment perturbations and control system errors.

2 Crop Growth Models

In order to apply model based control laws, we need to make use of crop growth models. In this paper, we consider two such models. The first is a growth and assimilation model, developed by the agricultural industry and used by the NASA Ames Research Center for previous ALSS studies. The second model is called the Energy Cascade model, which

takes a more mechanistic approach to predicting crop growth and overcomes some of the shortcomings of the Ames model. Both models assume a linear relation between light intensity and growth rates.

2.1 Ames Model

Originally developed by three agricultural companies (General Mills Inc., PhytoFarms of America, and CEA Technologies International, Inc.), this model has been utilized to study production systems for several crops including lettuce, spinach, wheat, and tomato. NASA's Ames Research Center has also applied the model towards design of environmental bioregenerative life support systems (4).

Relative growth rate (grams of new growth/grams of current growth on a dry or fresh weight basis) is predicted as a function of photosynthetic photon flux (PPF), CO_2 concentration, air temperature, plant production area, plant parameters (quantum use efficiency, canopy architecture), and initial plant dry or fresh weight:

$$G_i = \frac{CEa_iP_i}{W_i} \qquad a_i = 1 - e^{-k(W_i/S_i)} \tag{1}$$

where
G_i: relative growth rate (defined previously)
C: canopy quantum use efficiency [g biomass produced per mol intercepted PPF]
E: non-dimensional environment response surface, between 0 and 1, for air temperature and CO_2
P_i: photosynthetic photon flux integrated for simulation time increment [μmol m^{-2} time^{-1}]
W_i: dry or fresh crop weight [g plant^{-1}]
a_i: fraction of integrated photosynthetic photon flux intercepted by plant canopy
S_i: plant spacing [cm^2]
k: crop canopy constant
i: time increment [day]

The plant dry/fresh weight is determined as

$$W_{i+1} = W_i e^{G_i} \tag{2}$$

The model can be iterated on daily or smaller time increments. Control of crop growth can be achieved via manipulation of photoperiod and light intensity which contribute to the light integral for the given time step. The model is terminated at a user specified plant maturity date.

2.2 Energy Cascade Model

The energy cascade model (24) predicts crop productivity during plant growth and development based on a three step analysis involving:
1) light absorption L, where a fraction of photosynthetically active radiation available to the crop is absorbed by the canopy;
2) canopy quantum yield Q, the conversion of absorbed light energy into carbohydrate via photosynthesis;
3) carbon use efficiency U, the conversion of carbohydrate into plant biomass.

The model combines the above energy cascade process to predict gross and net photosynthesis (P_g and P_n), daytime respiration (R) and crop growth rate (CGR) as follows:

$$P_{gi} = P_{ni} + R_i \tag{3}$$

in which

$$P_{ni} = UQ_iL_iP_i \qquad R_i = (1-U)Q_iL_iP_i \tag{4}$$

To compute the daily crop growth rate (CGR), night time respiration needs to be taken into account. Thus CGR is equal to the daily net photosynthetic rate (H_iP_{ni}), where H_i is the photoperiod, minus plant respiration occurring during the dark ($(24-H_i)R_i$)

$$CGR_i = \beta\left(H_iP_{ni} - (24-H_i)R_i\right) \tag{5}$$

where
P_g, P_n, R: defined above with units [μmol CO_2 m^{-2} s^{-1}]
CGR: defined above with units [g m^{-2} d^{-1}]
β: conversion factor between moles CO_2 fixed by the plant and biomass
H: photoperiod [hr]

Dry weight is then calculated as:

$$W_{i+1} = W_i + CGR_i \tag{6}$$

where W_{i+1}: plant dry weight [g m^{-2}].

Unlike the Ames model, the Energy Cascade model also simulates the effect of senescence by assuming a linearly decreasing value for quantum use efficiency:

$$\begin{aligned} Q_i &= Q_{max} - \frac{(Q_{max}-Q_{min})(i-i_q)}{i_m - i_q} \quad \text{for } i > i_q \\ Q_i &= Q_{max} \qquad \text{for } i \le i_q \end{aligned} \tag{7}$$

where
Q_{max}: maximum quantum yield achievable for particular experiment
Q_{min}: smallest quantum yield observed for particular experiment
i_m: time to maturity
i_q: time at which Q begins to decline due to onset of senescence
i: time increment

Canopy growth and development are indirectly simulated with a linear increase in light absorption L until a constant maximum value of light absorption (L_{max}) is achieved according to

$$L_i = \frac{L_{max} * i}{i_l} \text{ for } i \le i_l \quad L_i = L_{max} \text{ for } i > i_l \tag{8}$$

where:
L_{max}: maximum light absorption at canopy closure (between 0 and 1)
i_l: time at which L_{max} is achieved

Model applications are restricted to the environmental ranges, plant cultivars, and planting densities from the data sets from which it was developed. Constant values are entered in the model for $L_{max}, Q_{max}, Q_{min}, U, i_l, i_q$, and i_m. The model accepts light intensity as an input.

3 Controller Development

In this section, we construct a model based crop growth controller. The input to the controller is taken as the PPF and the output is plant dry weight.

Consider a system described by the discrete time equations

$$x_{i+1} = [A_i]x_i + [B_i]u_i \qquad y_{i+1} = [C_{i+1}]x_{i+1} \tag{9}$$

in which i denotes the time step, x_i is the system vector of order n, describing the n states of the system, u_i is the control vector of order m, corresponding to m control inputs, and y_i is the output vector of p, denoting the measured states. The matrices $[A_i], [B_i]$ and $[C_i]$ describe the properties of the state, the relation of the controls to the state, and the relation between the measured values and the state variables, respectively.

The equations above can represent a discrete system, or they can be descriptive of a discretized model. In the latter case, the time increment should be selected such that the accuracy of the actual model is not compromised.

Let us denote the desired values of the output variables as $y_{di}, (i = 1, 2, ...)$. We first consider proportional control. Here, one designs the control input as

$$u_i = [K_i](y_{d_i} - y_i) - Z_i \tag{10}$$

where $[K_i]$ is the control gain matrix and $Z_i = [B_i]^{-1}(x_{d_{i+1}} - [A_i]x_{d_i})$. The gain matrix is selected such that the closed-loop system matrix $([A_i] - [B_i][K_i][C_i], i = 1, 2, ...)$ describes a stable system, that is, its eigenvalues lie within the unit circle. The procedures we use to select the control gains will be described later.

Another control approach is based on pointwise-optimal control (23). The objective of pointwise optimal control is to drive the system to a desired set of values and to do this by minimizing the difference between the measured variables and their desired quantities at each time step. Unlike conventional optimal control, which minimizes the difference between a desired state and an initial state over a period of time, pointwise optimal control does this at each time step. The result is a simpler, but a less sophisticated control law.

We wish to minimize the difference between y_{di} and y_i at each time increment. To this end, given the measurements at time step i, we predict the state at the next time increment $(i + 1)$ using Eq. (9) and we define a performance index as

$$J_{i+1} = e_{i+1}^T [H_{1_{i+1}}] e_{i+1} + u_i^T [H_{2_i}] u_i \tag{11}$$

where e_{i+1} is the error vector between the desired and actual values of the output,

$$\begin{aligned} e_{i+1} &= y_{d_{i+1}} - y_{i+1} = y_{d_{i+1}} - [C_{i+1}]x_{i+1} \\ &= y_{d_{i+1}} - [C_{i+1}]([A_i]x_i + [B_i]u_i) \end{aligned} \tag{12}$$

with $[H_1]$ and $[H_2]$ as error weighting matrices. Setting $[H_{2_i}]$ to zero implies that one can use as much control effort as needed, without regard to the amount used.

We take the derivative of J_{i+1} with respect to u_i

$$\frac{\partial J_{i+1}}{\partial u_i} = 2e_{i+1}^T [H_{1_{i+1}}] \frac{\partial e_{i+1}}{\partial u_i} + 2u_i^T [H_{2_i}] \tag{13}$$

where $\frac{\partial e_{i+1}}{\partial u_i} = [C_{i+1}][B_i]$. Setting Eq. (13) equal to zero and solving for u_i we obtain

$$u_i = [R_i]^{-1}(y_{d_{i+1}} - [C_{i+1}][A_i]x_i) \tag{14}$$

in which $[R_i] = [H_{2_i}] + [B_i]^T[C_{i+1}]^T[H_{1_{i+1}}][C_{i+1}][B_i]$. Equation (14) has x_i in it, which implies that if $[C_{i+1}]$ is not a square matrix (not as many measurements as there are states) an observer needs to be designed to estimate x_i from y_i. The same situation exists when proportional control is used.

Both control laws can be applied to the two crop models. Both mathematical models are of order $n = 1$ and there is one controller, $m = 1$. For now, we assume that the the state variable W_i, the dry weight, can be directly measured so that $[C_i]$ is a scalar and it is equal to 1. To obtain $[A_i]$ and $[B_i]$, which are also scalars, we recognize that both models must be in the state space form given by Eq.(9) (Note that the $[-]$ will now be dropped since the matrices are scalars for this application). This is now demonstrated using the Ames model.

In Eq. (3), dry weight is an exponential function of relative growth rate, G_i. The first-order Taylor series expansion of e^{G_i} is

$$W_{i+1} = W_i e^{G_i} \approx W_i(1 + G_i) \tag{15}$$

which is an accurate approximation when G_i is kept sufficiently small. This can be accomplished by reducing the model's time step to a 0.2 day period. Values for G_i simulated in the model do not exceed 0.7 per day. By utilizing a 0.2 day time period, the maximum simulated value is reduced to 0.14 and the resulting error due to linearization is 0.9%. Because we are designing a feedback controller and the dry weight W_i is measured at every time increment (one day), each approximation is carried out for one day only. That is, the control is to be applied at the end of each day of simulation, not at the 1/5 day time increment. Hence, errors associated with this approximation do not increase with time.

In Eq. (2), exponential of the plant dry weight divided by the plant spacing is computed to determine the fraction of light intercepted by the plant canopy. In this case, the linearization expansion can not be performed accurately because the dry weight continually increases throughout the simulation. This turns out to not be a drawback when designing the control law.

Combining Eqs. (1), (2), and (15) gives the following expression for crop dry weight:

$$W_{i+1} = W_i + CEa_iP_i \tag{16}$$

which now is in desired form, with $A_i = 1, B_i = CEa_i,\ C_i = 1, x_i = W_i$ and $u_i = P_i$.

4 Controller Implementation

In this section, we implement the two control laws described above for the Ames and Energy Cascade models. We consider the following issues:

a) The type of control law (proportional or pointwise-optimal);

b) The model on which the control design is based;

c) The model which is used to simulate crop dry weight;

d) Presence of measurement as well as control input errors.

For example, one procedure is to simulate the plant state via the Energy Cascade model, while designing the control law based on the Ames model. The reasoning behind this approach is to see if a controller based on one model can effectively control a different model. As the models of crop growth considered here are simplifications of complex phenomena, one needs to design a controller that has certain robustness features and one that will work with different models describing the same phenomena. Using more than one model to describe the same system is a common procedure for control system development (5) and is frequently done in the life sciences.

4.1 Applied Control Law Expressions

The weighting matrices in the pointwise-optimal control law become scalars $H_{1_{i+1}}$ and H_{2_i} when applied to the crop models considered here. Introducing all the coefficient terms used to derive the previous equation into Eq. (16), the control input for the Ames model becomes

$$u_i = P_i = \frac{W_{d_{i+1}} - W_i}{H_{2_i} + H_{1_{i+1}}(CEa_i)^2} \tag{17}$$

In general, the values for $H_{1_{i+1}}$ and H_{2_i} are selected by trial and error. Appropriate values for these matrices are discussed later on in this section. For the special case of no restrictions on the control effort, we can set H_{2i} to zero and selecting $H_{1_{i+1}} = 1/CEa_i$, we obtain

$$P_i = \frac{W_{d_{i+1}} - W_i}{CE(1 - e^{-kW_i/S_i})} \tag{18}$$

Note that the above equation can also be derived directly from Eq. (12), by prescribing that the difference $W_{d_{i+1}} - W_{i+1}$ be zero.

Basing the control design on the Energy Cascade model, and without putting a restriction on the control effort in the control design, we obtain a pointwise-optimal control law in the form

$$P_i = \frac{W_{d_{i+1}} - W_i}{BQ_iL_i(H_i + 24(U - 24))} \tag{19}$$

Finally, the proportional control law (Eq. (10)) as applied to the Ames model is

$$u_i = P_i = K_i(W_{d_i} - W_i) - \frac{W_{d_{i+1}} - W_d}{CEa_i} \tag{20}$$

A similar expression can be developed for the Energy Cascade model.

4.2 Identification of Control and Simulation Model

Simulations with the Energy Cascade and partially linearized Ames models were conducted prior to implementing feedback control. Baseline environmental conditions for simulation were set at a CO_2 concentration of 1200 ppm, a PPF level of 1400 μmol m^{-2} s^{-1}, a 23°C constant day/night temperature, photoperiod of 20 hours, and a production area of 14.3 cm^2 plant^{-1}. Model parameters were taken from (24) for the Energy Cascade and then fit to the Ames model (Table 1). Model simulations of wheat growth were similar until day 33 where productivity declined in the energy cascade model due to senescence (Figure 1). This result has important consequences when determining which model to use for simulation and for the control law.

Four separate simulations were performed to determine which model to use for control and for simulation. For example, one simulation used the Ames-based controller with the Energy Cascade model for dry weight prediction, while a second simulation used the Energy Cascade-based controller with the Energy Cascade model. Desired dry weights, $W_{d_{i+1}}$, were computed once for all four simulations using the Energy Cascade model under the baseline conditions discussed above with a setpoint PPF of 1400 μmol m^{-2} s^{-1}. The controller's response was restricted to a PPF range between 50 and 2000 μmol m^{-2} s^{-1} PPF, where

Energy Cascade		Ames	
L_{max}	0.93	C	1.12
Q_{max}	0.0625	k	100
Q_{min}	0.0125	E	0.85
U	0.68	W_o	0.001
i_l	12 days	S_i	14.3
i_q	33 days		
i_m	62 days		

Table 1: Parameters for Ames and Energy Cascade models.

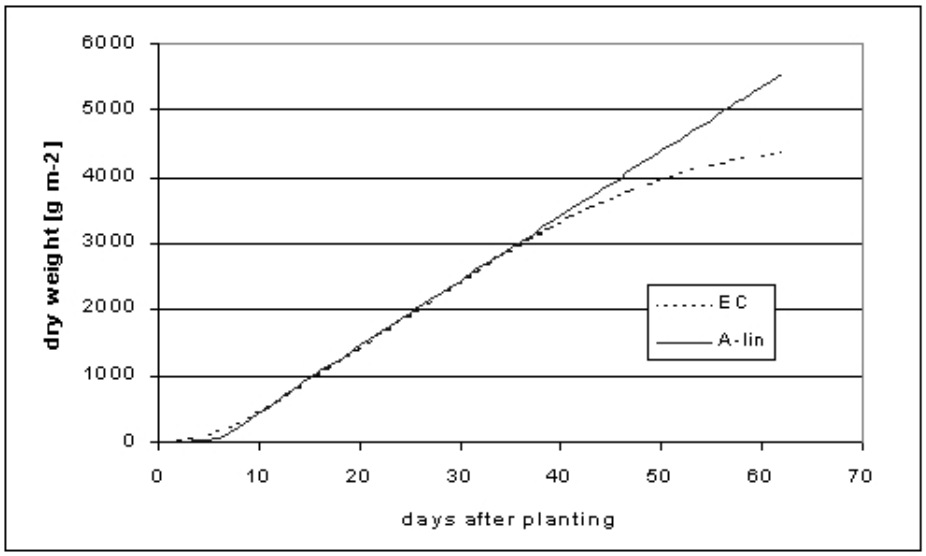

Figure 1: Comparison of Energy Cascade (EC) model versus partially linearized Ames model (A-lin) for wheat dry weight over time.

wheat response to changes in light intensity was assumed linear (19). Each simulation was judged on the controller's ability to achieve the desired plant weight values and feasibility of output PPF level; thus, no perturbations were included.

All four combinations were able to maintain the desired plant dry weights throughout the simulation. However, when the Ames model was used for simulation of crop growth, input PPF values were well off the nominal expected value of 1400. For example, when equation (19), the control law applied to the Energy Cascade model, was combined with the Ames model for plant simulations, PPF values following DAP 33 averaged 847 μmol m^{-2} s^{-1}. This unrealistic result occurred because the Ames model does not simulate the decline in plant productivity following the onset of senescence. The Ames model overpredicted plant dry weight, and the controller supplied lower PPF values to compensate.

Using either the Energy Cascade model or the Ames model for the control and the Energy Cascade model for the simulation produced the similar results. For brevity, our subsequent analysis is based on using the Ames-based control law (Eq. (18)) with the Energy Cascade

model for simulations.

4.3 Control Implementation

Simulations using the Ames-based pointwise-optimal control law (Eq. (18)) showed that the PPF oscillated wildly during different days of the simulation. This was because our control design did not weight the control effort. This is undesirable for two reasons: First, the control action is not smooth, which usually leads to high sensitivity to changes in parameters and instabilities in the control action. Secondly, such a control action will put large fluctuating demands on the power supply in the ALS environment, which may result in a reduction in power allocated to other components of the ALS. These considerations suggest that values for the control gain needed to be determined.

Simulations were conducted to determine parameters for proportional control, K_i, and weighing terms $H_{1_{i+1}}$, H_{2_i} for pointwise optimal control. The results were evaluated in terms of system response and required control effort. A normalized least squares criterion was introduced to quantify control effort and deviation from desired set points. The criterion evaluates the deviation in dry weight W_i as well as the control input PPF, and it has the form

$$\frac{LS_X = \sqrt{\sum_{i=1}^{62}(X_i - Xs_i)^2}}{LS_{XMAX}} \tag{21}$$

where X - dry weight W or light intensity PPF,
Xs_i - setpoint at time increment i, e.g., 1400 for $X = PPF$ or W_{d_i} for $X = W_i$
62 - number of days in simulation,
LS_{XMAX} - maximum least squares value observed from all simulations

For proportional control, the control gain K_i was selected so that the eigenvalue of the closed-loop system lay within the unit circle. This requires that values for K_i be negative. For pointwise-optimal control, $H_{1_{i+1}}$ was kept equal to $1/CEa_i$ as in Eq. (18), but H_{2_i} was set as a percentage of $H_{1_{i+1}}$. Separate simulations were run with proportional and pointwise-optimal control laws to determine appropriate constants for these parameters.

For both proportional and pointwise-optimal control simulations, least square values for system response were similar regardless of trial values selected. However, the amount of control effort varied greatly depending on the control gain selected. Figure 2 shows LS_{PPF} results for different proportional control gain values. It can be seen than a value of -0.6 (kept constant throughout the simulation) minimized PPF fluctuations. For pointwise-optimal, H_{2_i} set to 350% of $H_{1_{i+1}}$ minimized LS_{PPF}.

Using the best values of the control gain parameters, the predicted plant growth and input PPF for pointwise-optimal control and proportional control were compared. Table 2 summarizes the results for the least square values in plant growth and PPF for a variety of disturbances and for the two control laws considered. Disturbances consisted of ± 40%, 20% or 10% short term perturbations to the input PPF. Short term disturbances were implemented from day 11 to 20 for single disturbances and from days 11 to 15 and 31 to 35 for the double disturbances. Figure 3 compares control input over time between the two controllers for the case of no disturbances and the short term +10% case.

Using only the pointwise-optimal controller, four additional simulations were performed where ± 40% and 20% perturbations were maintained throughout the simulation. These simulations were conducted to determine the ability of the controller to respond to long term disturbances. Long term measurement errors (± 20% of W_i) were also input to the

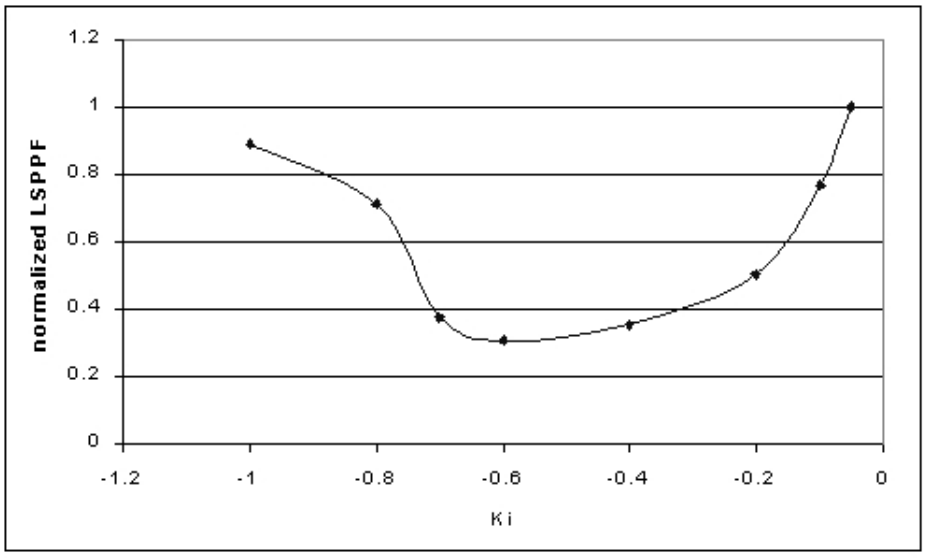

Figure 2: Effect of gain value for Ames-based proportional controller on control effort.

controller in separate simulations. Results are also summarized in Table 2. Figure 4 shows results from short and long term -40% perturbations respectively.

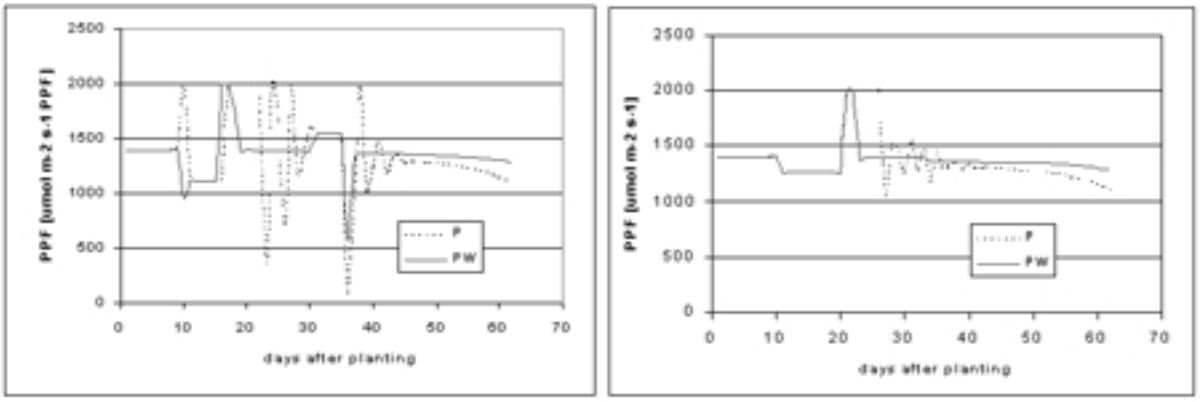

Figure 3: Control effort comparisons between proportional (P) and pointwise-optimal (PW) controllers. Examples shown are for -20%, +10% (left) and -10% short term perturbation (right).

5 Discussion

The results in Table 2 indicate that the proportional and pointwise-optimal controller performances are comparable in terms of maintaining desired plant dry weights. However, proportional control shows slightly more sensitivity to input disturbances as can be seen in Figure 3 and the larger LS_{PPF} values in Table 2. This higher sensitivity is a disadvantage.

scenario	**proportional**		**pointwise**		**pointwise**
	W_i	PPF_i	W_i	PPF_i	$\%deviation$
+40% PPF, 10 day	0.140	0.732	0.173	0.723	2 (8.6)
−40% PPF, 10 day	0.273	0.671	0.289	0.570	2 (9.2)
+20% PPF, 10 day	0.0749	0.463	0.128	0.473	2 (4.1)
−20% PPF, 10 day	0.156	0.512	0.188	0.345	2 (4.8)
+10% PPF, 10 day	0.0683	0.356	0.126	0.325	2 (2)
−10% PPF, 10 day	0.111	0.403	0.153	0.227	2 (2.6)
+20% , −10% 5 days	0.0665	0.365	0.139	0.376	2
−20% , +10% 5 days	0.098	0.653	0.152	0.341	2
+40% PPF, long	–	–	0.129	0.701	1.4
−40% PPF, long	–	–	1.0	0.825	19
+20% PPF, long	–	–	0.147	0.73	1.6
−20% PPF, long	–	–	0.229	0.742	2.5
+20% W_i, long	–	–	0.85	0.829	18
−20% W_i, long	–	–	0.954	0.972	22

Table 2: Normalized (0 to 1) least square values for plant growth W_i and PPF for different scenarios. Percent final deviation at maturity date presented for pointwise-optimal control only. Values in parenthesis are % deviation when no control action is applied.

Large fluctuations in input PPF may lead to a reduction in the energy supplied to other components of the ALS system and decrease longevity of the growth chamber lighting systems. The even distribution of energy and avoidance of excess variations in power demands will be an important concern as ALS subsystems are integrated (11). For this reason, the pointwise-optimal controller was shown to be a better controller choice for this application.

The short term disturbances introduced to the pointwise-optimal controller represent a range of some possible external perturbations to light intensity. The controller was able to compensate for all short term disturbances in PPF, as well as small (less than 20%) long term disturbances (Table 2 and Figure 4-right). However, for a long term perturbation of -40% PPF, predicted final dry weight ended 19% below its desired value. This occurred because PPF output was restricted due to the constraints set on the control law. Thus, the crop could not be restored to the original production schedule when a -40% disturbance was applied during the entire simulation (Figure 4-left). This implies that the simulation results are dependent on both the PPF setpoint and the PPF range constraints placed on controller response.

Table 2 also shows the resulting final dry weight errors for each short term scenario when no controller action was applied. That is, following the perturbation, PPF was set back to the nominal value of 1400 μmol m^{-2} s^{-1}. Errors ranged from about 10% to 2%. These deviations were reduced to less than 2% with the controller (Figure 4 shows the short term -40% result). It is worth noting that as the duration of perturbation increases, the deviations will increase. Thus, for short term and certain long term perturbations, utilization of a controller to restore the crops back to their original production schedule is a viable and necessary approach.

Useful real-time, non-destructive measurements of crop dry weight are not currently achievable. Hence, for real-time feedback control, an observation scheme needs to be developed to estimate the crop dry weight in a non-destructive way.

In such a situation, crew members would input environmental perturbations to an ob-

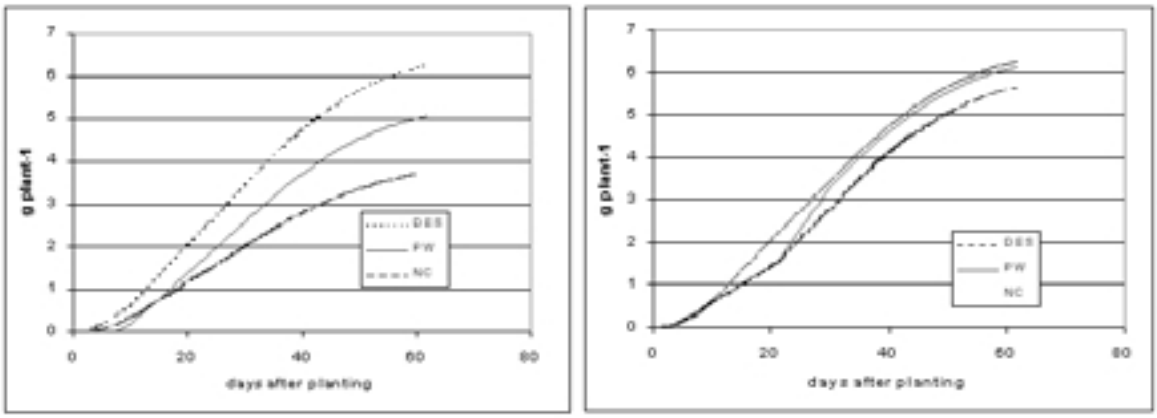

Figure 4: System response (W_i) from pointwise-optimal controller for -40% long term perturbation (left) and -40% short term perturbation (right). Simulated control values (PW) are compared with desired dry weights (DES) and results in which no control is applied (NC) to adjust for perturbation.

server to estimate the current dry weight W_i. This estimated dry weight would then be used as the input to the controller. To investigate the sensitivity of the control action to incorrect measurements of the dry weight, the controller was evaluated for when values for dry weight W_i in Eq. (16) were perturbed by $\pm$ 20%. As listed in Table 2, controller response is adversely affected by errors in the estimated dry weight. We conclude that an accurate estimation of W_i is critical to the controller's ability to compensate for environmental perturbations and is an important topic for research.

Ultimately, the development of dynamic controllers, such as the one presented here, for individual ALS processes will need to be considered as sub-systems are linked together. The simple method presented here is intended to outline one viable approach of developing such control for biomass production. There are several areas where the control design requires improvement. The controller is based on a single input, single output model. More realistic controllers will have to handle multiple inputs, including CO_2 concentration, temperature, photoperiod, and weightlessness. An improved model should also account for the nonlinear relationship between light intensity and growth rate. For example, constants that are fixed in the Energy Cascade model are actually dynamic functions of the environment. Values for Q_{max} and U depend on the current temperature, light intensity and CO_2 concentration, while photoperiod affects developmental parameters such as maturity and canopy closure dates. Incorporating these relationships into the controller will be important. Growth chamber experiments need to be developed to validate the results which are predicted by the controller. Finally, an observation scheme needs to be developed for estimating values of the dry crop weight.

6 Conclusions

A model-based controller is developed to maintain crop production schedules in advanced life support systems, where perturbations in light intensity and measurement of crop growth rates may be of concern. The control is applied to two plant growth models and wheat

is used as the crop. The response is evaluated with several 'what-if' scenarios including simulated short and long term errors in the input. The controller satisfactorily responds to small perturbations in controller inputs.

References

1. Aaslyng, J.M.; Ehler, N.; Karlsen, P.; Rosenqvist, E. Intelligrow: a component-based climate control system for decreasing greenhouse energy consumption. Acta Hort. 507:35-42; 1999.

2. Aikman, D.P. A procedure for optimizing carbon dioxide enrichment of a glasshouse tomato crop. J. Agric. Engng. Res. 63:171-184; 1996.

3. Barta, D.J.; Castillo, J.M.; Forston, R.E. The biomass production system for the bioregenerative planetary life support systems test complex: preliminary designs and considerations. SAE Technical Paper No. 1999-01-2188. Society of Automotive Engineers, Warrendale, PA; 1999.

4. Bates, M.E.; Bubenheim, D.L. Applications of process control to plant-based life support systems. SAE Technical Paper No. 972359. Society of Automotive Engineers, Warrendale, PA; 1999.

5. Blackwell C.C.; Blackwell, A.L. CELSS system control: Issues, methods, and directions. Adv. Space Res. 12(5):57-63; 1992.

6. Bugbee, B.G.; Salisbury, F.B. Current and potential productivity of wheat for a controlled environment life support system. Adv. Space Res. 9(8):5-15; 1989.

7. Bugbee, B.G.; Salisbury, F.B. Exploring the limits of crop productivity: Photosynthetic efficiency of wheat in high irradiance environments. Plant Physiology. 88:869-878; 1988.

8. Challa, H. Integration of explanatory and empirical crop models for greenhouse management support. Acta Hort. 507:107-116; 1999.

9. Challa, H.: van Straten, G. Optimal diurnal climate control in greenhouses as related to greenhouse management and crop requirements. In: Hashimoto, Y.; Bot, G.P.A.; Day, W.; Tantau, H.-J.,; Nonami, H., eds. The computerized greenhouse: Automatic control application in plant production. San Diego:Academic Press; 1993:119-138.

10. Chun, C.; Mitchell, C.A. Dynamic control of photosynthetic photon flux for lettuce production in CELSS. Acta Hort. 440:7-12; 1996.

11. Crawford, S.S.; Pawlowski, C.W.; Finn, C.K. Power management in regenerative life support systems using market-based control. SAE Technical Paper No. 2000-01-2259. Society of Automotive Engineers, Warrendale, PA; 2000.

12. Drysdale, A.; Fortson, R.; Stutte, G.; Mackowiak, C.; Sager, J.; Wheeler, R. Reliability of biological systems based on CBF data. SAE Technical Paper No. 961498. Society of Automotive Engineers, Warrendale, PA; 1996.

13. Eisenberg, J.N.; Maszle, D.R.; Pawlowski, C.W.; Auslander, D. Methodology for optimal plant growth strategies in life-support systems. J. Aero. Eng. 8(3):139-147; 1995.

14. Eisenberg, J.N.; Pawlowski, C.W.; Maszle, D.R.; Auslander, D. System issues for controlled ecological life support systems. Life Support and Biosphere Sci. 1:141-157; 1995.

15. Henninger, D.L. Life Support Systems Research at the Johnson Space Center. In: Ming, D.W.; Henninger, D.L., eds. Lunar base agriculture: Soils for plant growth. Amer. Society of Agronomy; ISBN: 0891181008; 1989:173-191.

16. Hoff, J.E.; Howe, J.M.; Mitchell, C.A. Nutritional and cultural aspects of plant species selection for a regenerative life support system. NASA-CR Publication 166324; 1982.

17. Hogan, J.A.; Cowan, R.M.; Joshi, J.A.; Strom, P.F.; Finstein, M.S. On the development of advanced life support systems maximally reliant on biological systems. SAE Technical Paper No. 981535. Society of Automotive Engineers, Warrendale, PA; 1998.

18. Hopper, D.A.; Stutte, G.W.; McCormack, A.; Barta, D.J.; Heins, R.D.; Erwin, J.E.; Tibbitts, T.W. Crop Growth Requirements. In: Langhans, R.W.; Tibbitts, T.W., eds. Plant growth chamber handbook. North Central Regional Research Publication No. 340. Iowa State University; 1997:217-225.

19. Loomis, R.S.; Conner, D.J. Crop ecology: productivity and management in agricultural systems. Cambridge Univ. Press; 1996:257-288.

20. MacElroy, R.D.; Tremor, J.; Bubenheim, D.L. (1989). The CELSS research program: A brief review of recent activities. In: Ming, D.W.; Henninger, D.L., eds. Lunar base agriculture: Soils for plant growth. Amer. Society of Agronomy; ISBN: 0891181008; 1989:165-171.

21. Seginer, I.; Buwalda, F.; van Stratten, G. Nitrate concentration in greenhouse lettuce: A modeling study. Acta Hort. 507:141-148; 1998.

22. Seginer, I; Oslovich, I. Optimal spacing and cultivation intensity for an industrialized crop. Agricultural Systems. 62:143-157; 1999.

23. Tadikonda, S.S.K.; Baruh, H. Pointwise-optimal control of robotic manipulators. J. of Dynamic Systems, Measurement and Control. 110:210-213, 1988.

24. Volk, T.; Bugbee, B.; Wheeler, R.M. An approach to crop modeling with the energy cascade. Life Support and Biosphere Sci. 1:119-127.

Biographical Sketches

David Fleisher is an interdisciplinary Ph.D. candidate in Bioresource Engineering, Plant Science and Mechanical and Aerospace Engineering. He holds B.S. and M.S. degrees in Bioresource Engineering and a B.A. in Philosophy from Rutgers University. His research interests include crop modeling, systems analysis, and control.

Haim Baruh is an associate professor in Mechanical and Aerospace Engineering. He has a M.S. and Ph.D. in Engineering Mechanics from Virginia Polytechnic Institute and State

University. His research interests include modeling and control of elastic structures, control of agricultural systems, and dynamics.